Original Article

MOLECULAR METABOLISM

Dorsal raphe serotonergic neurons suppress feeding through redundant forebrain circuits

Iltan Aklan [1], Nilufer Sayar-Atasoy [1], Fei Deng [3], Hyojin Kim [1], Yavuz Yavuz [1,2], Jacob Rysted [1], Connor Laule [1], Debbie Davis [1], Yulong Li [3], Deniz Atasoy [1,4,5,*]

ABSTRACT

Objective: Serotonin (5HT) is a well-known anorexigenic molecule, and 5HT neurons of dorsal raphe nucleus (DRN) have been implicated in suppression of feeding; however, the downstream circuitry is poorly understood. Here we explored major projections of DRN^{5HT} neurons for their capacity to modulate feeding.

Methods: We used optogenetics to selectively activate DRN^{5HT} axonal projections in hypothalamic and extrahypothalamic areas and monitored food intake. We next used fiber photometry to image the activity dynamics of DRN^{5HT} axons and 5HT levels in projection areas in response feeding and metabolic hormones. Finally, we used electrophysiology to determine how DRN^{5HT} axons affect downstream neuron activity.

Results: We found that selective activation of DRN^{5HT} axons in (DRN^{5HT} → LH) and (DRN^{5HT} → BNST) suppresses feeding whereas activating medial hypothalamic projections has no effect. Using *in vivo* imaging, we found that food access and satiety hormones activate DRN^{5HT} projections to LH where they also rapidly increase extracellular 5HT levels. Optogenetic mapping revealed that DRN^{5HT} → LH^{vGAT} and DRN^{5HT} → LH^{vGlut2} connections are primarily inhibitory and excitatory respectively. Further, in addition to its direct action on LH neurons, we found that 5HT suppresses GABA release from presynaptic terminals arriving from AgRP neurons.

Conclusions: These findings define functionally redundant forebrain circuits through which DRN^{5HT} neurons suppress feeding and reveal that these projections can be modulated by metabolic hormones.

Keywords Serotonin; 5HT; Feeding; Dorsal raphe; Satiety

1. INTRODUCTION

Obesity and eating disorders have been on steady rise over the last few decades and constitute significant burden to overall healthcare system. Serotonergic dysregulation has been implicated in both obesity and anorexia nervosa (AN). Overactive serotonergic neurons have been linked to AN and consistently, multiple human GWAS studies have identified polymorphisms in 5HT receptor (5HTR) subunits from AN patients [1–4]. Conversely, obesity decreases serotonin levels in hypothalamus [5,6].

Serotonin is a well characterized anorexigenic molecule [7,8]. Selective activation of DRN^{5HT} neurons was causally linked to appetite suppression [9,10]. Consistently, cFos activity mapping showed increased DRN neuronal activity with feeding [11,12]. However, the downstream pathways through which DRN^{5HT} axons mediate their anorexic effects are poorly understood.

Within the forebrain, DRN^{5HT} neurons make widespread projections; however, much of the effort to understand serotonergic regulation of feeding has focused on mediobasal hypothalamic structures. Arcuate nucleus (ARC) harbors appetite regulating neurons that express various 5HTR subtypes, whose activation would be expected to reduce feeding [13,14]. Direct intracranial injections of 5HT or fenfluramine into various hypothalamic nuclei have been shown to suppress feeding [15,16]. For example, paraventricular hypothalamus (PVN) is one of the most sensitive sites to anorexigenic effect of 5HT injections. However, both retrograde and anterograde anatomical studies showed that projections from DRN^{5HT} neurons to these regions are so sparse that it is not clear whether these axons have functional significance [17–19]. Conversely, DRN^{5HT} neurons make dense projections to lateral hypothalamus (LH) [18],and feeding increases LH 5HT levels [20–22]. However, fenfluramine injections into this region were reported not to suppress appetite [16]. Thus, it remains to be seen whether LH and other forebrain projections of DRN^{5HT} neurons have functional relevance to feeding. Furthermore, it is also unknown whether and how these pathways respond to metabolic hormones that regulate energy homeostasis.

Here, we examined the major hypothalamic and extrahypothalamic projections of DRN^{5HT} neurons and identified LH and bed nucleus of the stria terminalis (BNST) as mediators of their anorexigenic phenotype.

[1]Department of Neuroscience and Pharmacology, Roy J. and Lucille A. Carver College of Medicine, University of Iowa, Iowa City, IA, USA [2]Department of Physiology, School of Medicine, Yeditepe University, Istanbul, Turkey [3]State Key Laboratory of Membrane Biology, Peking University School of Life Sciences, Beijing 100871, China [4]Iowa Neuroscience Institute, Roy J. and Lucille A. Carver College of Medicine, University of Iowa, Iowa City, IA, USA [5]Fraternal Order of Eagles Diabetes Research Center (FOEDRC), Roy J. and Lucille A. Carver College of Medicine, University of Iowa, Iowa City, IA, USA

*Corresponding author. Department of Pharmacology, Carver College of Medicine, University of Iowa, 51 Newton Rd, Iowa City, IA 52242, USA. Fax: +1 319 335 8930. E-mail: deniz-atasoy@uiowa.edu (D. Atasoy).

Received June 16, 2022 • Revision received December 4, 2022 • Accepted January 13, 2023 • Available online 20 January 2023

https://doi.org/10.1016/j.molmet.2023.101676

We showed acute 5HT dynamics in LH and BNST and Ca^{2+} level changes in DRN and its projection to LH and BNST in response to feeding and metabolic hormones.

2. METHODS

2.1. Animals

Mice used in this study were housed on 12-h light and dark cycle at 20 °C—24 °C, having *ad libitum* access to standard chow food and water unless noted otherwise. *Cre*-recombinase-expressing lines *Sert-cre* (B6.129(Cg)-*Slc6a4*$^{tm1(cre)Xz}$/J Jackson Labs Stock 014554) and *Agrp-ires-cre* (Agrp$^{tm1(cre)Lowl}$, Jackson Labs Stock 012899) were back-crossed with C57BL/6 (Jackson Labs Stock 000664) for maintenance. Electrophysiological and behavioral studies were performed with 6—12 weeks old male and female mice. Animal care and experimental procedures were approved by The University of Iowa.

2.2. Stereotaxic surgeries

2.2.1. rAAV injections

Stereotaxic surgeries were performed as described previously [50]. Briefly, 1—2 months old mice were anaesthetized with isoflurane in the stereotaxic instrument (David Kopf instruments, Tujunga-CA). Skull was exposed with an incision on the scalp and drilled for injection. ~200—600 nL virus was injected intracranially using a pulled glass pipette (Drummond Scientific, Wiretrol, Broomall-PA) with 50 μm tip diameter. Viral injections were performed on DRN (bregma: −3.80 mm, midline: ±0 mm, dorsal surface: −2.50 mm) and ARC (bregma: −1.15 mm, midline: ±0.30 mm, dorsal surface: −5.70 mm) by a micromanipulator (Narishige, East Meadow, NY), allowing 10 min time for the injection. The $5HT_{2h}$ sensor injections were conducted on LH (bregma: −1.15 mm, midline: ±1.00 mm, dorsal surface: −5.10 mm), or BNST (bregma: +0.62 mm, midline: ±0.42 mm, dorsal surface: −4.45 mm). Optic fiber placement was performed after removing the pipette. At least 4—6 weeks were given for animal recovery and transgene and sensor expression before further experiments.

2.2.2. Optical fiber placement

For the optogenetic stimulation, the ferrule capped optical fiber (200 μm core diameter, NA = 0.50, ThorLabs) was implanted above LH (bregma: −1.15 mm, midline: ±1.00 mm, dorsal surface: −4.80), PVN (bregma: −0.60 mm, midline: ±0 mm, dorsal surface: −4.45), and BNST (bregma: +0.62 mm, midline: ±0.42 mm, dorsal surface: −4.15). For the fiber photometry recordings, we implanted the optical fiber (400 μm core diameter, NA = 0.48, Thorlabs) over LH (bregma: −1.15 mm, midline: ±1.00 mm, dorsal surface: −4.90), BNST (bregma: +0.62 mm, midline: ±0.42 mm, dorsal surface: −4.25), or DRN (bregma: −3.80 mm, midline: ±0 mm, dorsal surface: −2.30 mm).The ferrule tip locations were positioned to be approximately 300 μm above the area for the photostimulation and 100—200 μm above the area for the fiber photometry. Ferrule placements were performed following the injections and held with dental cement.

2.3. Behavioral studies

2.3.1. Mapping of DR^{SERT} neuronal projections

To address this, DRN^{SERT} neurons were transfected with *AAV-FLEX-GFP* (Addgene 51502) virus in *Sert-cre* mice. After 4—6 weeks for the recovery and the transgene expression, the brain was enucleated as a following of cardiac perfusion. The brains were fixed in 4% of paraformaldehyde (PFA) solution for 4 h. Then, PFA was replaced with 30% sucrose solution. After a few days, 100 μm of brain slices starting from DRN to forebrain were obtained by using Vibratome. Next, brain slices were stained with GFP antibody (Abcam Ab290, 1:1000 dilution). After immunostaining, they were imaged by Slide Scanner Microscope (Olympus) and shown in Figure S1.

2.3.2. Food intake during optogenetic stimulation

For optogenetic stimulation, DRN^{SERT} neurons were transfected with *AAV5-FLEX-ChR2-EYFP* (Addgene 20298) or control *AAV5-FLEX-tdTomato* (Addgene 28306). Following recovery time, animals were single housed in custom-made plexiglass cages. In the cages, animals had cotton bedding and free access to chow food and water. Before the optogenetic stimulation, animals were handled for 3—4 days by being tethered to the optic fiber for acclimatization. Baseline food intake was measured for 4—5 days with tethered animals, without stimulation. Stimulation was performed at dark onset to determine anorexigenic effect. In Figure 1, the pre-stimulation food consumption was measured between ZT10 and ZT12. Stimulation (20 Hz, 18 mW, 10 ms pulse width, and 1 s on-3 s off) was done between ZT12 and ZT0. Food intake was measured at 2 h, 4 h, 12 h time points. To determine effect of stimulation on refeeding, animals were fasted for 18 h, stimulation was started 15 min before food access; then, the food intake was measured at 30 min, 1 h, and 2 h. Same experiment, without the stimulation was performed as control experiment. Light onset photo-stimulation where ZT2-4, ZT4-6 and ZT6-8 were accepted as pre-stimulation, stimulation, post-stimulation, respectively. Food intake was measured at the end of each time interval.

2.3.3. Real-time place preference, elevated plus maze, open field assays

Real time place preference is performed as described previously [32], briefly: DRN$^{SERT:ChR2}$ → LH and DRN$^{SERT:tDTom}$ → LH mice were put in a custom-made behavior chamber (25 × 50 × 25 cm), where one half of the chamber was coupled with constant 10 Hz photostimulation and no photostimulation was applied on the other half of the chamber. Mice were traced with CCD camera by EthoVision15 for 30 min. Time spent on each side of the chamber was recorded.

Elevated plus maze: Plus maze setup with two open arms (5 × 35 cm) and two closed arms (5 × 35 × 20 cm) was elevated for 35 cm. DR$^{SERT:ChR2}$ → LH and DR$^{SERT:tDTom}$ → LH mice were placed in the center of the maze, facing towards the open arm and were photostimulated and monitored for 5 min. The tests were recorded with a CCD camera and analyzed with EthoVision15 software.

Open field assay: DR$^{SERT:ChR2}$ → LH and DR$^{SERT:tDTom}$ → LH mice were placed in an open field test chamber (40 × 40 × 40 cm) and stimulated with the pulse protocol for 10 min. The assay was traced with a CCD camera and analyzed by EthoVision software.

2.4. Electrophysiology

P60—P80 mice were sacrificed 4—6 weeks after intracranial ChR2-eYFP or GFP expressing virus injection, to ensure sufficient expression in distant terminals or soma. Brains were immersed in a 95% O_2/5% CO_2 aerated ice-cold cutting solution including (in mM): 234 sucrose, 28 $NaHCO_3$, 7 dextrose, 2.5 KCl, 7 $MgCl_2$, 0.5 $CaCl_2$, 1 sodium ascorbate, 3 sodium pyruvate and, 1.25 NaH_2PO_4, and 300 μm thick fresh slices containing the hypothalamus were obtained with vibratome and transferred to 95% O_2/5% CO_2 aerated artificial cerebrospinal fluid (aCSF) containing (in mM): 119 NaCl, 25 $NaHCO_3$, 11 dextrose, 2.5 KCl, 1.25 $MgCl_2$, 2 $CaCl_2$, and 1.25 NaH_2PO_4. The sections were incubated in this solution for approximately 30 min in the

room temperature and then, placed in the recording chamber. Cell-attached and whole-cell patch clamp recordings were performed on LH, PVN and BNST neurons using electrodes with 4–5 MΩ tip resistances. aCSF was used as the pipette solution for cell-attached recordings. MultiClamp 700B Amplifier (Molecular Devices, San Jose, CA) and Axon™ pCLAMP™ 10.6 software (Molecular Devices, San Jose, CA) were used to obtain and analyze data. Blue light is delivered through objective using light pulses generated by CoolLED. LH, PVN, and BNST recordings were performed from randomly selected cells in *Sert-cre* mice using loose seal. Multiple sweeps were collected for each cell. Change in firing rate during photostimulation was defined as at least 25% consistent increase (or decrease) in average firing rate during photostimulation (30 s–60 s) compared to prestimulation baseline period (0 s–30 s) across sweeps. In *Agrp-ires-cre* mice, whole cell voltage clamp recordings (using cesium chloride based pipette solution) from ARC^{AgRP} → LH and ARC^{AgRP} → PVN terminals were performed before and after adding of CP-94253 (200 nM 5-HT1B agonist) into bath of the acute slice to show the impact of 5-HT1B agonist on ARC^{AgRP} → LH and ARC^{AgRP} → PVN synaptic connections (respectively, Figures 4 and Figure S6). To test the effect of added CP-94253, 5–10 min baseline was recorded, and drug was perfused in bath solution. Traces in which average post-drug activity remain within ±20% of baseline regarded as unresponsive.

2.5. In vivo fiber photometry recording and analysis

For Ca^{2+} imaging, DRN^{SERT} neurons were transduced with *AAV-CAG-DIO-GCaMP7s* (Addgene 104495) for somatic from DRN imaging and with *AAV-FLEX-AxonGCaMP6s* (Addgene 112010) for axon terminal imaging from LH or BNST. For 5HT imaging, forward AAV virus expressing $5HT_{2h}$ (WZ-biosciences) was stereotaxically delivered to LH or BNST using above coordinates. Following surgery recovery, animals were single housed in custom made plexiglass cages with free access to chow food and cotton bedding and allowed for 1–2 days of acclimatization to the cage. Then, the mice were tethered to the fiber optic fiber (400 μm core, 0.48 NA, bundled fibers, Doric Lenses). The connection area between the implanted ferrule and the optic cable were covered with black ceramic mating sleeves (Thorlabs). Mice were allowed 3–4 days to acclimate being tethered before the fiber photometry experiments. Briefly, fiber photometry was recorded at 3 Hz sampling rate, using Doric FP Bundle Imager (Doric Lenses). Light intensity for each wavelength at the end of the tip was set to be approximately 30–50 μW. We recorded Ca^{2+} or 5HT level changes in response to food and satiety cocktails after 16 h fasting and to the ghrelin hormone under fed condition. For the analysis, we fitted the isosbestic signal (405 nm) to the $Ca^{2+}/5HT_{2h}$ dependent (465 nm) signal using the linear least squares fit in a custom MATLAB script. Then, we calculated the ΔF/F as (465 nm − fitted 405 nm)/(fitted 465 nm). To account for the inter-animal differences in signal intensities, we calculated the z-scores for the baseline period which was determined as the 5–10 min before the administration of object/food and saline/metabolic hormones. After the post hoc analysis, mice were eliminated by the off-target fiber tip location and virus or sensor expression.

2.6. Single cell rt-PCR

Following the patch-clamp recordings, cytoplasmic contents of the neurons were aspirated into patch-clamp pipettes and then were transferred into microtubes with RNA extraction buffer. Total RNA extraction (PicoPure RNA Extraction Kit, Thermo Fisher Scientific, Waltham, MA), and first strand cDNA synthesis (RevertAid First Strand cDNA Synthesis Kit, Thermo Fisher Scientific, Waltham, MA), were followed with PCR in 20 μl reaction buffers, containing 1 μl of the single cell cDNA and the specific primers for Vgat mRNA (Forward: 5′-TCCTGAAATCGGAAGGCGAG-3′, Reverse: 5′-CAGCACGAACATGCCCT-GAA-3′), Vglut2 mRNA (Forward: 5′-CAGCAAGGTTGGCATGTTGT-3′, Reverse: 5′-ACTGCAAGCACCAAGAAGGA-3′), and ACTB mRNA (Forward:5′-AAGGCCAACCGTGAAAAGAT-3, Reverse:5′-GTGGTACGACCA-GAGGCATAC-3′). A second round of PCR was performed with 0.5 μl of the products of first round. Final products were then monitored with 2% agarose gels for the presence/absence of the genes.

2.7. Immunohistochemistry, fixed tissue imaging and post hoc analysis

Anesthetized mice were transcardially perfused with 4% paraformaldehyde in phosphate buffer saline (0.1 M pH 7.4) and decapitated. Brains were collected, incubated in the same fixative for 4 h and transferred to 30% sucrose solution overnight. 100 μm brain sections were collected with vibratome and the sections were blocked in PBS-T containing 5% normal goat serum for 1 h at room temperature. Blocking solution with the primary antibody (anti-GFP, 1:1000, Abcam Ab290) was then added on the sections. Following an overnight incubation at +4 °C, sections were rinsed with PBS-T. Secondary antibody (goat anti-rabbit IgG (H + L) Alexa Flour 488, 1:500, Invitrogen) was added on the sections and incubated for 1 h at room temperature. Sections were then rinsed, transferred to microscope slides and mounted with Fluoromount (Sigma F4680). Imaging was performed by confocal microscopy (FV3000 Confocal Scanning Microscope, Olympus) and slide scanner microscope (VS200 Slide View, Olympus).

2.8. Statistical analysis

All results were represented as Mean ± SEM. Differences between two groups were tested with paired and unpaired Student's t-tests. For more than 2 groups, the statistical comparison was measured by two-way repeated measures ANOVA using Prism 8.1 (GraphPad Software Inc.). N represents mice or neuron numbers as indicated for each experiment. A p-value <0.05 was considered to be statistically significant. Custom MATLAB codes are available upon request.

3. RESULTS

3.1. DRN^{5HT} neurons inhibit appetite through redundant forebrain pathways

Serotonergic neurons of DRN make extensive projections throughout the forebrain [18]. We first verified the extent of these projections using anterograde tracing. For this, DRN of *Sert-cre* mice were transduced with *AAV-FLEX-GFP* and sections from various appetite-related forebrain areas were examined (Figure S1). In agreement with previous reports, we observed robust projections to lateral hypothalamus (LH) and bed nucleus of stria terminalis (BNST) among other regions. Of note, there was limited innervation in medial hypothalamic areas known to be involved in appetite regulation. Specifically, sparse projections were observed in paraventricular hypothalamic nucleus (PVN) and extremely sparse innervation was found in the arcuate nucleus of hypothalamus (ARC).

To determine whether these projections have the capacity to influence appetite, we prepared three separate sets of mice and selectively stimulated DRN^{SERT} axonal projections to LH, BNST and PVN using optogenetics (Figure 1A). Stimulation of DRN^{SERT} → LH and DRN^{SERT} → BNST projections caused significant reduction in dark onset feeding, whereas DRN^{SERT} → PVN had no impact in mice with *ad libitum* food access (Figure 1B–D). DRN^{SERT} → LH projection was also effective at suppressing refeeding in fasted mice but did not change

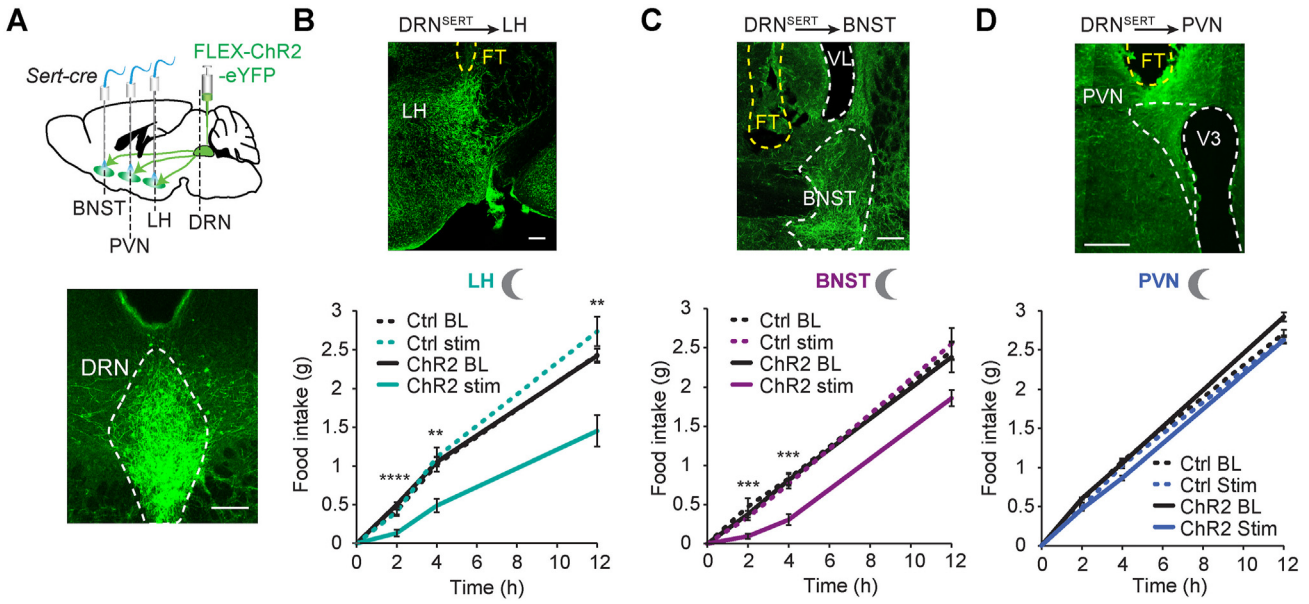

Figure 1: Stimulation of DRN^{SERT} axons suppress feeding through multiple forebrain targets. (A) Schematic diagram for stimulation of serotonergic axonal projections from DRN to LH, BNST, and PVN (upper). ChR2 expression in DRN^{SERT} neurons in *Sert-cre* mice (lower). (B–D) Representative photomicrograph showing ChR2 expressing DRN^{SERT} axons and dark onset food intake in response to DR$^{SERT:ChR2}$ axonal photostimulation in LH (B), BNST (C), and PVN (D) of *ad libitum*-fed mice areas. N = 8–18 mice, Two-way repeated measures ANOVA; **p < 0.01, ***p < 0.001, ****p < 0.0001; (FT, fiber track, yellow dashed line, scale: 200 μm). (For interpretation of the references to color in this figure legend, the reader is referred to the Web version of this article.)

ad libitum food intake in daytime. Conversely, DRN^{SERT} → BNST stimulation did not influence refeeding response in fasted mice (Figure S2). These results suggest that LH and BNST are downstream targets of DRN^{SERT} neurons in mediating its anorexigenic effect.

3.2. DRN^{5HT} neurons respond to food and metabolic signals in a projection specific manner

Although the DRN serotonergic axons to LH and BNST have the capacity to suppress feeding, it is unclear whether these projections are part of physiological satiety mechanisms and recruited by satiation. To understand *in vivo* DRN^{SERT} neuronal activity dynamics during feeding, we performed Ca^{2+} based fiber photometry imaging from *Sert-cre* mice in which DRN was transduced with *AAV-CAG-DIO-GCaMP7s*. Mice were overnight fasted and given access either to an inedible object or chow food (Figure 2A). DRN^{SERT} neuronal activity spiked briefly with access to both object or food; however, this activity rapidly went back to baseline levels within a few seconds as refeeding continued (Figure 2B,C). We also tested whether DRN^{SERT} neurons respond to metabolic hormones. Intraperitoneal injections of neither a cocktail of satiety hormones (CCK, amylin and PYY) nor the hunger hormone ghrelin caused a significant change in overall activity (Figures 2D, E and S3).

Since fiber photometry gives an average read-out of cumulative DRN^{SERT} neuronal activity, lack of food-specific response might be due to response-heterogeneity among labeled neurons. Thus, we decided to image activity of individual DRN^{SERT} neuronal projections. We focused on projections to LH and BNST because selective activation of these projections was sufficient to suppress feeding. For this, we expressed axon targeted GCaMP6s in DRN^{SERT} neurons and placed an optical fiber over the LH or BNST (Figures 2F and S4A). We found that DRN^{SERT} → LH axonal activity rapidly increased with food access (Figure 2G,H). Although there was a trend in DRN^{SERT} → BNST projection, this was not statistically significant over object access (Figure S4B and C). Conversely, satiety hormones rapidly increased Ca^{2+} activity in the DRN axonal terminals in both LH and BNST (Figures 2I, J and S4D, E), but there was no response to ghrelin (Figure S3). These results show that activity of DRN^{SERT} neuronal projections in LH increases with food, and both LH and BNST terminals respond to satiety hormones.

3.3. 5HT levels in LH and BNST increase with satiety

To better understand how food and metabolic hormones affect serotonergic dynamics in the identified downstream targets, we used a fluorescent 5HT sensor, GRAB-5HT$_{2h}$ in LH and BNST. A viral vector carrying GRAB-5HT$_{2h}$ was stereotaxically delivered into LH or BNST, over which an optical fiber was placed for *in vivo* imaging (Figures 2K and S4F). Notably, food access caused a rapid and significant increase in fluorescence signals in both LH and BNST, suggesting that 5HT levels quickly rise with feeding (Figures 2L, M and S4G, H). Similarly, intraperitoneal injection of satiety cocktail caused a significant increase in both regions (Figures 2N, O and S4I, J). Neither region had detectable change in 5HT levels in response to ghrelin injection (Figure S3). Collectively, these results show that serotonergic input onto LH and BNST target regions is sensitive to food access as well as metabolic hormones signaling satiety.

3.4. DRN^{SERT} → LH projection is aversive and anxiogenic

Our results suggest that both LH and BNST downstream targets receive increased serotonergic drive in response to satiety hormones and feeding. Although these findings suggest that this pathway might be involved in physiological satiety, reduction in food intake can also occur if these projections are associated with negative valence. Therefore, we tested anxiogenic properties of DRN downstream targets by focusing on DRN^{SERT} → LH connection. We performed a close loop active place-preference assay to test whether DRN^{SERT} axons in LH is aversive or rewarding. We found that mice strongly avoided the stimulated side,

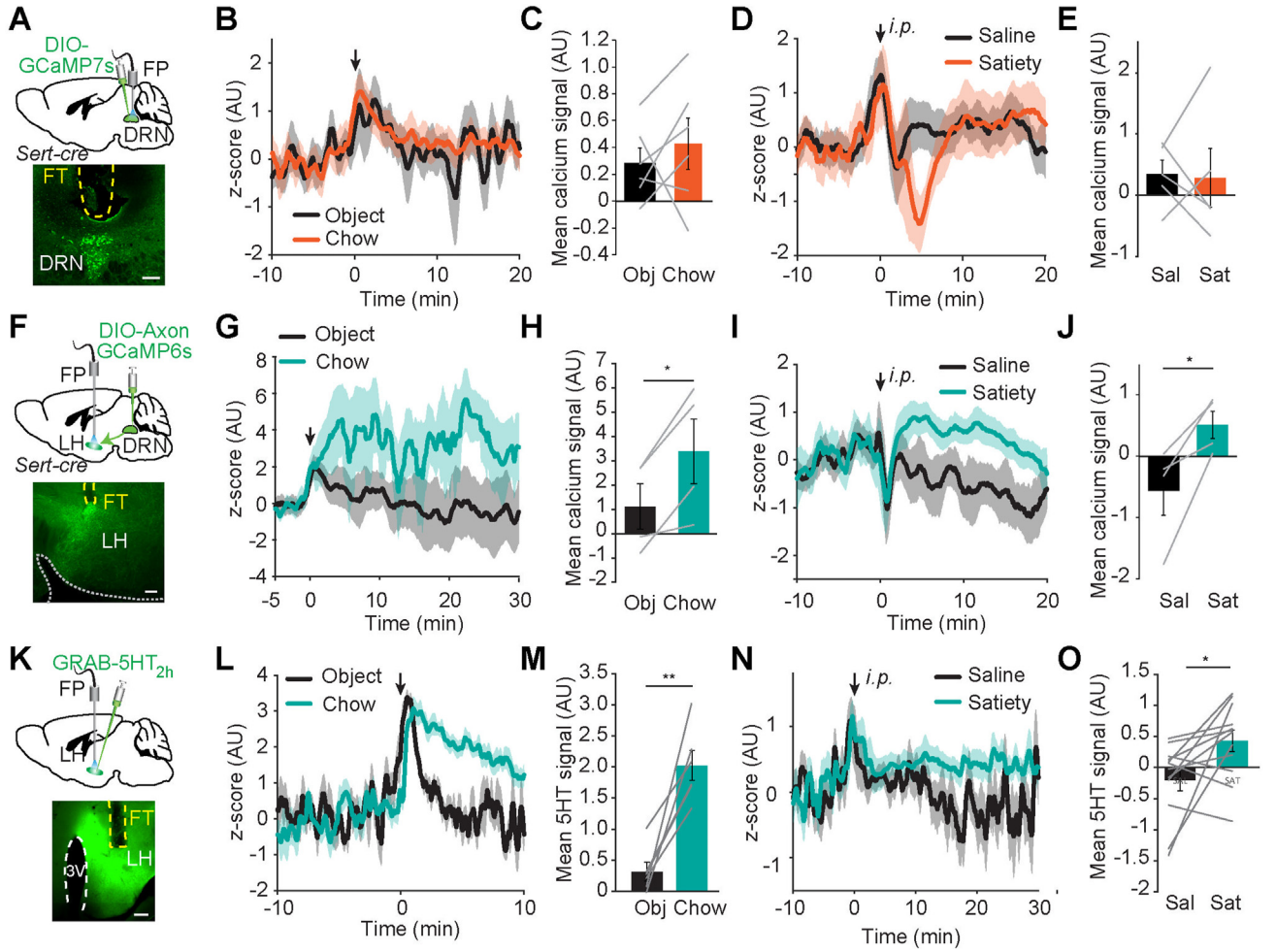

Figure 2: Food and satiety hormones alter activity in DRN^{SERT} → LH axonal terminals and 5HT levels in LH. (A) Schematic and representative image of GCaMP7s expressing DRN^{SERT} soma and optic fiber placement above DRN. (B,C) Average fiber photometry traces of DRN GCaMP7s activity in response to chow food and object presentation under fasting condition (B) and quantification of mean signals (C). (D,E) Same as in (B,C) except GCaMP7s response to intraperitoneal (i.p.) injection of saline or a cocktail of satiety hormones (3 μg/kg CCK, 10 μg/kg PYY, 10 μg/kg Amylin) were measured under fasting condition. (F–J) Same as (A–E) except, DRN^{SERT} neurons were transduced with AxonGCaMP6s and fiber was placed on LH. (K) Schematic of *in vivo* 5HT measurement and representative image of 5HT$_{2h}$ sensor expression in LH. (L,M) Average fiber photometry trace of 5HT levels in LH in response to chow food and object presentation under fasting condition (L) and quantification of mean 5HT$_{2h}$ signal (M). (N,O) Same as in (B,C) except 5HT$_{2h}$ response to intraperitoneal (i.p.) injection of saline or a cocktail of satiety hormones (3 μg/kg CCK, 10 μg/kg PYY, 10 μg/kg Amylin) were measured under fasting condition. (FT, fiber track, yellow dashed line, N = 4–6 mice/group, *p < 0.05, Student's t-test, scale: 300 μm). . (For interpretation of the references to color in this figure legend, the reader is referred to the Web version of this article.)

suggesting that activity in this projection is aversive (Figure S5A–C). Consistently, in both elevated plus maze and open field assays we observed increased anxiety-like behavior (Figure S5D–G). Thus, aversive properties of DRN^{SERT} → LH projection may contribute to the hypophagia observed with its optogenetic stimulation.

3.5. DRN^{SERT} axons elicit heterogeneous response in target areas

To determine the downstream circuitry mediating anorexigenic effect of DRN neurons, we performed acute slice recordings from innervated areas, LH, BNST and PVN, while stimulating DRN^{SERT} axons (Figure 3A). Blind loose-seal recordings from both LH and BNST showed heterogeneous response profiles in spontaneous firing rates of target neurons such that some neurons increased their activity, while others were suppressed in response to DRN^{SERT} axonal photostimulation; however, majority of neurons in both regions were unresponsive (Figure 3B–F). Consistent with the weak innervation, we did not detect any change in the activity of PVN neurons.

Previous studies showed that LH contains both orexigenic and anorexigenic populations [23,24]. To determine the molecular identity of LH neurons targeted by DRN^{SERT} axons, we performed single cell rt-PCR from neurons that changed activity in response to photostimulation. LH neurons activated by DRN^{SERT} axons were all glutamatergic, whereas those suppressed were a mixed population, mostly being vGAT+ (Figure 3G–I). Together, these results show a complex innervation profile of DRN^{SERT} axons in LH with multiple neuronal subtypes targeted and differentially modulated.

3.6. Multiple routes of 5HT mediated modulation of LH neurons

To understand cellular basis of interaction between DRN^{SERT} axons and LH neurons, we performed whole cell voltage clamp recordings. We found that LH neurons did not show any time-locked synaptic currents in response to DRN^{SERT} axonal photostimulation, suggesting that DRN^{SERT} axons do not make any direct synaptic contact, which is in striking contrast to the effect on spontaneous activity we observed with

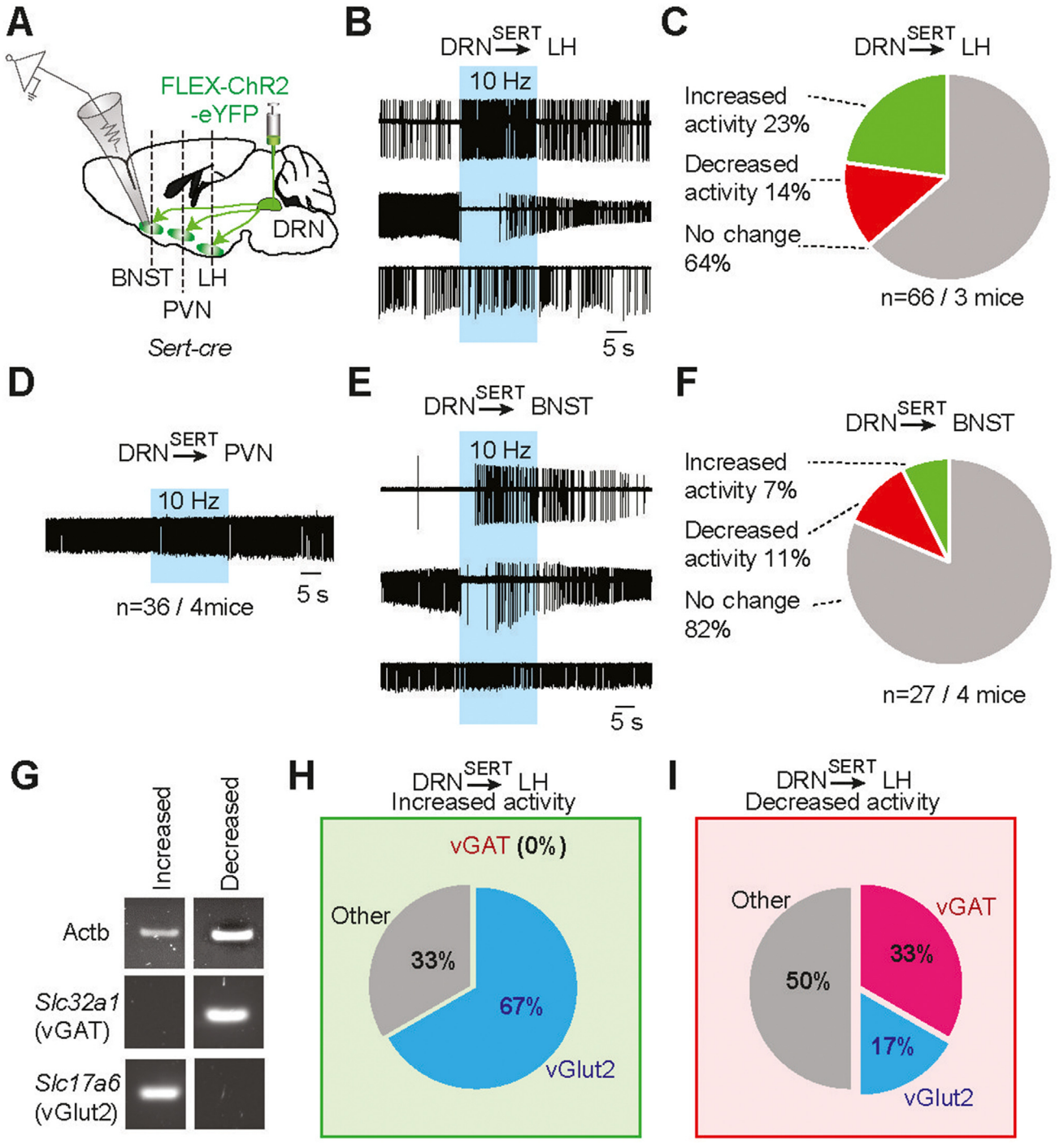

Figure 3: Photostimulation of DRN^{SERT} axons elicit heterogenous response in downstream targets. (A) Schematic diagram for evaluating the impact of DRN^{SERT} axonal photostimulation on LH, BNST, and PVN neurons. (B,C) Representative loose seal recording traces for various response patterns in action currents observed from randomly recorded LH neurons upon stimulation of DR$^{SERT:ChR2}$ → LH axons (B). Summary pie chart depicting relative fraction of different responses in firing rates observed from recorded LH neurons (C). No synaptic blockers were present. (D) Representative loose seal recording traces to show no response in action currents observed from randomly recorded PVN neurons upon stimulation of DRN$^{SERT:ChR2}$ → PVN axons. (E,F) Same as in (B,C) except recorded from BNST neurons. (G–I) Single cell RT-PCR characterization of a subset of LH neurons that responded to DRN^{SERT} axonal photostimulation from (C). Representative image of gel electrophoresis outcomes of RT-PCR for two different cell types (G): vGAT+, vGlut2−, and vGAT−:vGlut2+. Summary pie chart of characterization of neurons in LH responded with increased (H) and decreased (I) activity pattern in response to stimulation of DR$^{SERT:ChR2}$ → LH axons (H, n = 6 neurons each).

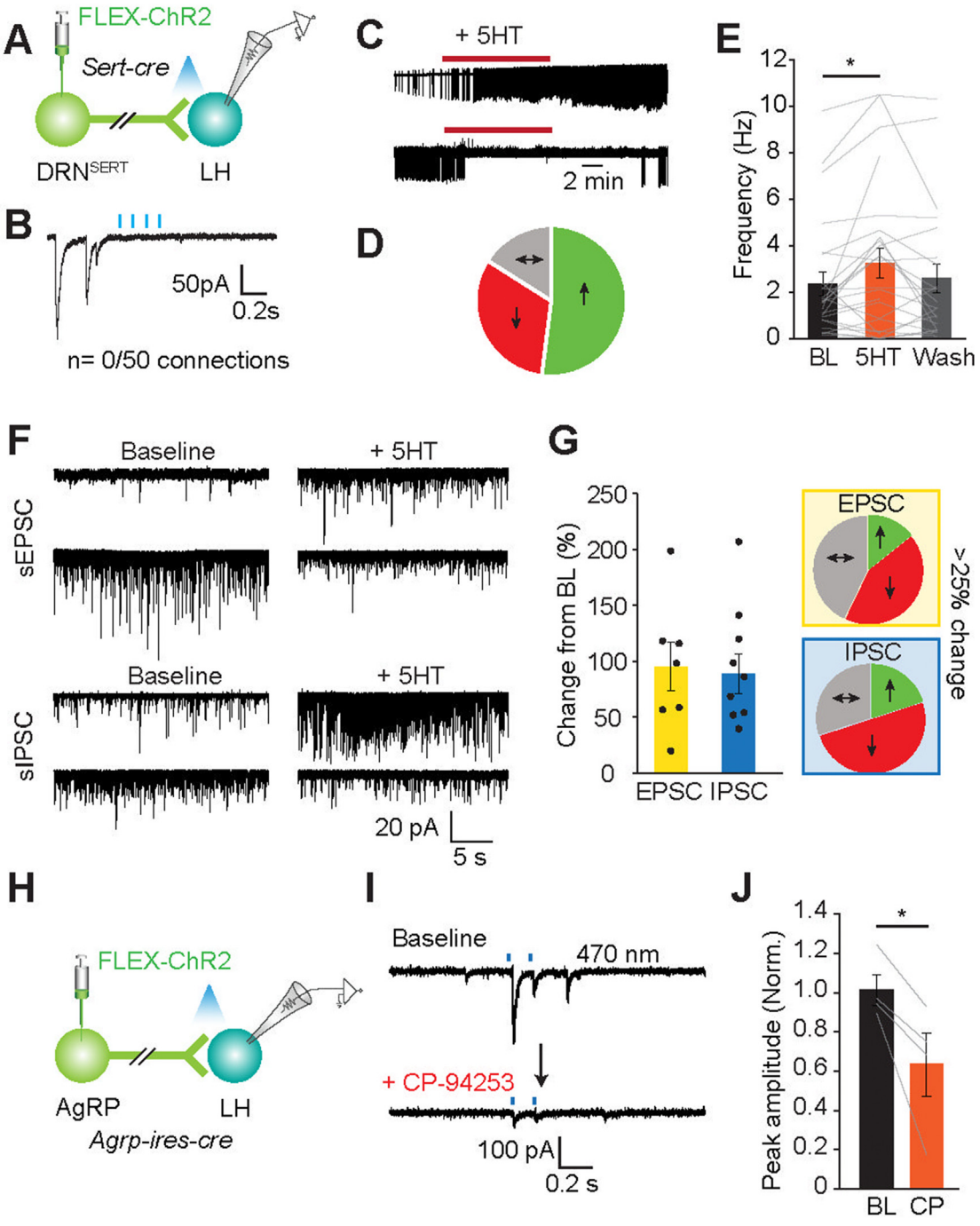

Figure 4: DRN^{SERT} axons do not make direct synaptic connections onto LH neurons but 5HT can modulate LH neuron activity. (A,B) Schematic for ChR2 assisted interrogation of DRN^{SERT} → LH synaptic connection in *Sert-cre* mice (A) and representative whole cell recordings from LH neurons during photoactivation of DRN^{SERT} terminals during. (C–E) Representative loose seal recording traces for response patterns in action currents observed from randomly recorded LH neurons upon 5HT perfusion in the presence of synaptic blockers (C). Summary pie chart of various activity pattern (D) and bar graph quantification of change in firing rate before 5HT addition (BL), after 5HT addition (5HT), and after washout of the drug (Wash) (E). (F,G) Same as in (C–E) except whole cell voltage clamp recordings performed and change in synaptic currents onto LH neurons were quantified in response to 5HT addition. Note that 5HT alters synaptic input in various ways (F). Bar graph and summary pie chart depicting different responses in EPSC and IPSC records in comparison to BL in response to 5HT administration (G). (H–J) 5HT1B agonist (CP94253) inhibits AgRP synaptic terminal in LH. Schematic ChR2 assisted interrogation of ARC^{AgRP} → LH synaptic connection in *Agrp-ires-cre* mice (H). Representative whole cell voltage clamp traces from LH neurons that respond to AgRP axon photostimulation; baseline activity and impact of CP-94253 on AgRP-mediated synaptic currents (I). Bar graph of normalized peak amplitude in baseline and after CP94253 administration (J) ($n = 4$ neurons, $^{*}p < 0.05$).

loose-seal recordings (Figure 4A,B). Thus, instead of synaptic connections, DRN^{SERT} axons likely modulate LH neurons through the released 5HT. To confirm this, we performed loose seal recordings from LH neurons and evaluated the effect of 5HT perfusion on spontaneous activity. Consistent with DRN^{SERT} axonal stimulation, pharmacologic application of 5HT caused a mixed reaction on LH neuronal activity with excitation being the primary response (Figure 4C–E). It is likely that 5HT directly acts on LH neurons since these recordings were performed in the presence of synaptic blockers. However, 5HT can also modulate synaptic input through presynaptic 5HT receptors. Indeed, whole cell recordings from LH neurons confirmed that both sEPSC and sIPSC responses are sensitive to extracellular 5HT levels with the dominant response being downregulation of synaptic input (Figure 4F,G). These results suggest that DRN^{SERT} axons likely modulate LH neuronal activity through released 5HT, which can act directly on LH neurons or downregulate its synaptic input.

3.7. 5HT directly suppresses GABA release from AgRP terminals

A key appetite-regulating synaptic input onto LH is derived from ARC^{AgRP} neurons [25]. Serotonergic suppression of AgRP neuron activity has been described before [14]; however, we could not detect any direct DRN^{SERT} axonal innervation to the ARC (Figure S1). It is possible that serotonergic pathway might regulate the AgRP neuron output in its target regions such as the LH. To test this possibility, we transduced ARC^{AgRP} neurons with ChR2 and performed whole cell recordings from LH neurons. Consistent with previous reports, we identified direct GABAergic synaptic connections from ARC^{AgRP} → LH [26]. Perfusion of CP94253, agonist for 5HT1BR which is the subtype expressed on AgRP neurons, significantly suppressed magnitude of ARC^{AgRP} synaptic currents onto LH neurons (Figure 4H–J). Although photoactivation of DRN^{SERT} → PVN projection did not change food intake, given dense axonal innervation of PVN by AgRP axons, we tested whether these terminals are also 5HT sensitive. Similar to AgRP connections to LH, we found that AgRP → PVN connection is significantly suppressed by CP94253, suggesting that other AgRP target areas may also be modulated by 5HT (Figure S6). These findings support that 5HT suppresses AgRP neuron output at the level of pre-synaptic GABA release.

4. DISCUSSION

Here, we identified two forebrain regions, LH and BNST, through which DRN^{SERT} efferents acutely suppress feeding. Both food access and peripheral satiety hormones changed activity of DRN^{SERT} axonal terminals in these regions. Consistently, using fluorescent 5HT sensor we found that extracellular 5HT levels parallel the increased DRN^{SERT} axonal activity. These findings are in line with earlier dialysis studies showing increased 5HT levels in LH in response to food and CCK and that DRN projections to LH is anorexigenic [20,27–29] and provides evidence that increased serotonergic activity extends to BNST as well. Together with axonal imaging, our results suggest that DRN is a key brain region supplying nutrient-related serotonergic input to these regions to suppress food intake.

In striking contrast with projection measurements, neither food nor satiety hormones caused a detectable change in DRN^{SERT} activity when measured from soma. Although there was a transient response to food this was not specific since non-edible object caused a similar change. These results are inconsistent with a recent report showing increased GCaMP based activity in DRN 5HT neurons [10]. The underlying reason for the discrepancy is unclear but it might be related to the difference in recording duration, which was shorter in our case. Alternatively, DRN 5HT neurons may respond heterogeneously to food and satiety hormones such that cumulative fiber photometry response would become undetectable. Finally, food access and satiety hormones may directly act on synaptic terminals of DRN^{SERT} neurons and modulate its output rather than increasing somatic firing rate. Regardless of the mechanism, our findings confirm food and satiety hormone responsiveness of DRN^{SERT} neurons and extend earlier observations by providing temporal kinetics and projection specific effects.

Serotonergic regulation of feeding through LH has been poorly understood. 5HT was reported to inhibit orexin and MCH neurons [30,31] in LH; however, these neurons have limited impact on satiety [32–34]. Our recordings from blindly targeted LH neurons suggested that dominant response to pharmacologic 5HT application is excitation. This appears to be mediated through both direct effect on LH neuronal soma and modulation of synaptic inputs. Optogenetic activation of DRN^{SERT} axons elicited heterogeneous response in LH. Whole cell recordings suggested that this interaction is not mediated by fast synaptic transmission as we failed to detect any direct synaptic connection. Nevertheless, we cannot rule out the possibility of GABA or glutamate corelease that may act through their respective metabotropic receptors. Our single cell rt-PCR experiments suggested selective activation of glutamatergic and inhibition of GABAergic LH neurons by DRN^{SERT} axons. Given that LH GABA neurons stimulate appetite, and vGlut2 neurons inhibit feeding [23,24], the heterogeneous neuronal response profile observed upon DR^{SERT} → LH photostimulation is consistent its hypophagic effect.

Serotonin receptors are extensively expressed in both LH and BNST [35–38]. Heterogeneity of the target neuronal response in slice recordings is likely mediated by direct serotonin action on multiple receptor subtypes as well as presynaptic modulation. We found that BNST is another major DRN target capable of suppressing appetite. Recent studies identified BNST as a relay hub receiving orexigenic input from ARC and tuberal nucleus (TN) [25,39]. BNST, in turn, provides input back to ARC, LH and DRN [40–43] to modulate feeding. Alternatively, DRN^{SERT} → BNST input may promote hypophagia through stimulation of aversive state and anxiety [44]. Interestingly, even though BNST 5HT levels are highly responsive to food, this was not observed with axonGCaMP imaging from DRN terminals in BNST, suggesting that other serotonergic input may also contribute to food induced 5HT release in this region. However, DR^{SERT} → BNST axonal terminals were responsive to satiety hormones and its optogenetic activation was anorexigenic.

Given the stimulating effect of satiety hormones on DRN^{SERT} axons and 5HT release, we also examined whether the opposite is true for the hunger hormone ghrelin. Indeed, it was shown that intra-DRN ghrelin injection is sufficient to increase feeding [45]. In addition, based on polysynaptic inhibition of DRN^{SERT} neurons by AgRP axons, one of the primary targets of ghrelin, it is predicted that ghrelin may inhibit DRN^{SERT} activity and 5HT levels [9,46,47]. However, we found that neither soma nor projection recordings from DRN^{SERT} neurons showed any response to ghrelin injections, suggesting that ghrelin induced appetite and suppression of thermogenesis may not be through DRN suppression.

The interaction between serotonergic pathway and mediobasal hypothalamic appetite circuits is thought to be bidirectional. ARC^{AgRP} and ARC^{POMC} neurons are known to express 5HT receptor subtypes that inhibit or activate them respectively. Recently, using anterograde functional circuit mapping, AgRP and POMC neurons were shown to receive direct input from DRN^{Tph2} expressing neurons [10]. However, with *Sert-cre* line to anterogradely label DRN serotonergic axons, we found that innervation in the ARC was extremely sparse. Our results are in line with retrograde viral tracing from AgRP neurons, which also failed to identify somatic labeling in DRN neurons [17]. One possibility

is that distal dendritic branches AgRP and POMC neurons might be exposed to DRN^{SERT} axons. Indeed, such distal modulation was shown for excitatory inputs [48]. In contrast to the limited ARC innervation, DRN^{SERT} neurons project heavily to some of the brain areas also innervated by AgRP projections. Notably, we found that CP94253 directly inhibited synaptic currents elicited by AgRP axons in LH and PVN [49], suggesting Gi-coupled 5HT1B-R on AgRP neurons directly inhibit output at presynaptic level (Figure S7). Thus, serotonergic input from DRN and potentially from other sources may also alter target neuronal activity through modulation of release from AgRP axon terminals.

In summary, we identified novel downstream forebrain circuits through which DRN^{SERT} neurons suppress feeding. Given that hyperactivation of serotonergic neurons has been linked to anorexia [1,2], and obesity suppresses serotonin levels in hypothalamus [5,6], future research is warranted to determine how the activity in these circuits maladapt to altered 5HT levels in order to refine potential therapeutic targets.

AUTHOR CONTRIBUTIONS

IA performed behavioral and imaging experiments, surgeries; NSA performed data analysis and prepared figures, performed genotyping and scRT-PCR and prepared MATLAB code for data acquisition and analysis; IA, YY performed electrophysiological recordings; HK, IA, JR performed imaging; HK, IA, JR, NSA, CL contributed to *post hoc* analysis; DA conceived experiments; DA, IA, and NSA prepared the manuscript.

DATA AVAILABILITY

Data will be made available on request.

ACKNOWLEDGMENTS

This work is supported by NIH to D.A. R01DK126740.

CONFLICT OF INTEREST

The authors declare no competing financial interests.

APPENDIX A. SUPPLEMENTARY DATA

Supplementary data to this article can be found online at https://doi.org/10.1016/j.molmet.2023.101676.

REFERENCES

[1] Kaye WH, Gwirtsman HE, George DT, Ebert MH. Altered serotonin activity in anorexia nervosa after long-term weight restoration. Does elevated cerebrospinal fluid 5-hydroxyindoleacetic acid level correlate with rigid and obsessive behavior? Arch Gen Psychiatry 1991;48(6):556–62.

[2] Cai X, Liu H, Feng B, Yu M, He Y, Liu H, et al. A D2 to D1 shift in dopaminergic inputs to midbrain 5-HT neurons causes anorexia in mice. Nat Neurosci 2022;25(5):646–58.

[3] Bergen AW, van den Bree MB, Yeager M, Welch R, Ganjei JK, Haque K, et al. Candidate genes for anorexia nervosa in the 1p33-36 linkage region: serotonin 1D and delta opioid receptor loci exhibit significant association to anorexia nervosa. Mol Psychiatry 2003;8(4):397–406.

[4] Brown KM, Bujac SR, Mann ET, Campbell DA, Stubbins MJ, Blundell JE. Further evidence of association of OPRD1 & HTR1D polymorphisms with susceptibility to anorexia nervosa. Biol Psychiatry 2007;61(3):367–73.

[5] Routh VH, Stern JS, Horwitz BA. Serotonergic activity is depressed in the ventromedial hypothalamic nucleus of 12-day-old obese Zucker rats. Am J Physiol 1994;267(3 Pt 2):R712–9.

[6] Banas SM, Rouch C, Kassis N, Markaki EM, Gerozissis K. A dietary fat excess alters metabolic and neuroendocrine responses before the onset of metabolic diseases. Cell Mol Neurobiol 2009;29(2):157–68.

[7] Bhave VM, Nectow AR. The dorsal raphe nucleus in the control of energy balance. Trends Neurosci 2021;44(12):946–60.

[8] van Galen KA, Ter Horst KW, Serlie MJ. Serotonin, food intake, and obesity. Obes Rev 2021;22(7):e13210.

[9] Nectow AR, Schneeberger M, Zhang H, Field BC, Renier N, Azevedo E, et al. Identification of a brainstem circuit controlling feeding. Cell 2017;170(3):429–442 e11.

[10] He Y, Cai X, Liu H, Conde KM, Xu P, Li Y, et al. 5-HT recruits distinct neurocircuits to inhibit hunger-driven and non-hunger-driven feeding. Mol Psychiatry 2021;26(12):7211–24.

[11] Wu Q, Lemus MB, Stark R, Bayliss JA, Reichenbach A, Lockie SH, et al. The temporal pattern of cfos activation in hypothalamic, cortical, and brainstem nuclei in response to fasting and refeeding in male mice. Endocrinology 2014;155(3):840–53.

[12] Flores RA, da Silva ES, Ribas AS, Taschetto APD, Zampieri TT, Donato J, et al. Evaluation of food intake and Fos expression in serotonergic neurons of raphe nuclei after intracerebroventricular injection of adrenaline in free-feeding rats. Brain Res 2018;1678:153–63.

[13] Xu Y, Jones JE, Lauzon DA, Anderson JG, Balthasar N, Heisler LK, et al. A serotonin and melanocortin circuit mediates D-fenfluramine anorexia. J Neurosci 2010;30(44):14630–4.

[14] Heisler LK, Jobst EE, Sutton GM, Zhou L, Borok E, Thornton-Jones Z, et al. Serotonin reciprocally regulates melanocortin neurons to modulate food intake. Neuron 2006;51(2):239–49.

[15] Shor-Posner G, Grinker JA, Marinescu C, Brown O, Leibowitz SF. Hypothalamic serotonin in the control of meal patterns and macronutrient selection. Brain Res Bull 1986;17(5):663–71.

[16] Weiss GF, Rogacki N, Fueg A, Buchen D, Leibowitz SF. Impact of hypothalamic d-norfenfluramine and peripheral d-fenfluramine injection on macronutrient intake in the rat. Brain Res Bull 1990;25(6):849–59.

[17] Wang D, He X, Zhao Z, Feng Q, Lin R, Sun Y, et al. Whole-brain mapping of the direct inputs and axonal projections of POMC and AgRP neurons. Front Neuroanat 2015;9:40.

[18] Ren J, Isakova A, Friedmann D, Zeng J, Grutzner SM, Pun A, et al. Single-cell transcriptomes and whole-brain projections of serotonin neurons in the mouse dorsal and median raphe nuclei. Elife 2019;8.

[19] Sawchenko PE, Swanson LW, Steinbusch HW, Verhofstad AA. The distribution and cells of origin of serotonergic inputs to the paraventricular and supraoptic nuclei of the rat. Brain Res 1983;277(2):355–60.

[20] Schwartz DH, Hernandez L, Hoebel BG. Serotonin release in lateral and medial hypothalamus during feeding and its anticipation. Brain Res Bull 1990;25(6):797–802.

[21] Mori RC, Guimaraes RB, Nascimento CM, Ribeiro EB. Lateral hypothalamic serotonergic responsiveness to food intake in rat obesity as measured by microdialysis. Can J Physiol Pharmacol 1999;77(4):286–92.

[22] Hoebel BG, Hernandez L, Schwartz DH, Mark GP, Hunter GA. Microdialysis studies of brain norepinephrine, serotonin, and dopamine release during ingestive behavior. Theoretical and clinical implications. Ann N Y Acad Sci 1989;575:171–91. discussion 192-3.

[23] Stamatakis AM, Van Swieten M, Basiri ML, Blair GA, Kantak P, Stuber GD. Lateral hypothalamic area glutamatergic neurons and their projections to the lateral habenula regulate feeding and reward. J Neurosci 2016;36(2):302–11.

[24] Jennings JH, Ung RL, Resendez SL, Stamatakis AM, Taylor JG, Huang J, et al. Visualizing hypothalamic network dynamics for appetitive and consummatory behaviors. Cell 2015;160(3):516–27.

[25] Betley JN, Cao ZF, Ritola KD, Sternson SM. Parallel, redundant circuit organization for homeostatic control of feeding behavior. Cell 2013;155(6):1337–50.
[26] Garau C, Blomeley C, Burdakov D. Orexin neurons and inhibitory Agrp → orexin circuits guide spatial exploration in mice. J Physiol 2020;598(19):4371–83.
[27] Boden PR, Woodruff GN, Pinnock RD. Pharmacology of a cholecystokinin receptor on 5-hydroxytryptamine neurones in the dorsal raphe of the rat brain. Br J Pharmacol 1991;102(3):635–8.
[28] Voigt JP, Sohr R, Fink H. CCK-8S facilitates 5-HT release in the rat hypothalamus. Pharmacol Biochem Behav 1998;59(1):179–82.
[29] Schneeberger M, Brice NL, Pellegrino K, Parolari L, Shaked JT, Page KJ, et al. Pharmacological targeting of glutamatergic neurons within the brainstem for weight reduction. Nat Metab 2022;4(11):1495–513.
[30] van den Pol AN, Acuna-Goycolea C, Clark KR, Ghosh PK. Physiological properties of hypothalamic MCH neurons identified with selective expression of reporter gene after recombinant virus infection. Neuron 2004;42(4):635–52.
[31] Muraki Y, Yamanaka A, Tsujino N, Kilduff TS, Goto K, Sakurai T. Serotonergic regulation of the orexin/hypocretin neurons through the 5-HT1A receptor. J Neurosci 2004;24(32):7159–66.
[32] Dilsiz P, Aklan I, Sayar Atasoy N, Yavuz Y, Filiz G, Koksalar F, et al. MCH neuron activity is sufficient for reward and reinforces feeding. Neuroendocrinology 2020;110(3–4):258–70.
[33] Viskaitis P, Arnold M, Garau C, Jensen LT, Fugger L, Peleg-Raibstein D, et al. Ingested non-essential amino acids recruit brain orexin cells to suppress eating in mice. Curr Biol 2022;32(8):1812–1821 e4.
[34] Inutsuka A, Inui A, Tabuchi S, Tsunematsu T, Lazarus M, Yamanaka A. Concurrent and robust regulation of feeding behaviors and metabolism by orexin neurons. Neuropharmacology 2014;85:451–60.
[35] Jalewa J, Joshi A, McGinnity TM, Prasad G, Wong-Lin K, Holscher C. Neural circuit interactions between the dorsal raphe nucleus and the lateral hypothalamus: an experimental and computational study. PLoS One 2014;9(2):e88003.
[36] Lorrain DS, Riolo JV, Matuszewich L, Hull EM. Lateral hypothalamic serotonin inhibits nucleus accumbens dopamine: implications for sexual satiety. J Neurosci 1999;19(17):7648–52.
[37] Hazra R, Guo JD, Dabrowska J, Rainnie DG. Differential distribution of serotonin receptor subtypes in BNST(ALG) neurons: modulation by unpredictable shock stress. Neuroscience 2012;225:9–21.
[38] Garcia-Garcia AL, Canetta S, Stujenske JM, Burghardt NS, Ansorge MS, Dranovsky A, et al. Serotonin inputs to the dorsal BNST modulate anxiety in a 5-HT(1A) receptor-dependent manner. Mol Psychiatry 2018;23(10):1990–7.
[39] Luo SX, Huang J, Li Q, Mohammad H, Lee CY, Krishna K, et al. Regulation of feeding by somatostatin neurons in the tuberal nucleus. Science 2018;361(6397):76–81.
[40] Smith MA, Choudhury AI, Glegola JA, Viskaitis P, Irvine EE, de Campos Silva PCC, et al. Extrahypothalamic GABAergic nociceptin-expressing neurons regulate AgRP neuron activity to control feeding behavior. J Clin Investig 2020;130(1):126–42.
[41] Jennings JH, Rizzi G, Stamatakis AM, Ung RL, Stuber GD. The inhibitory circuit architecture of the lateral hypothalamus orchestrates feeding. Science 2013;341(6153):1517–21.
[42] Hao S, Yang H, Wang X, He Y, Xu H, Wu X, et al. The lateral hypothalamic and BNST GABAergic projections to the anterior ventrolateral periaqueductal gray regulate feeding. Cell Rep 2019;28(3):616–624 e5.
[43] Wang Y, Kim J, Schmit MB, Cho TS, Fang C, Cai H. A bed nucleus of stria terminalis microcircuit regulating inflammation-associated modulation of feeding. Nat Commun 2019;10(1):2769.
[44] Marcinkiewcz CA, Mazzone CM, D'Agostino G, Halladay LR, Hardaway JA, DiBerto JF, et al. Serotonin engages an anxiety and fear-promoting circuit in the extended amygdala. Nature 2016;537(7618):97–101.
[45] Carlini VP, Varas MM, Cragnolini AB, Schioth HB, Scimonelli TN, de Barioglio SR. Differential role of the hippocampus, amygdala, and dorsal raphe nucleus in regulating feeding, memory, and anxiety-like behavioral responses to ghrelin. Biochem Biophys Res Commun 2004;313(3):635–41.
[46] Han Y, Xia G, Srisai D, Meng F, He Y, Ran Y, et al. Deciphering an AgRP-serotoninergic neural circuit in distinct control of energy metabolism from feeding. Nat Commun 2021;12(1):3525.
[47] Bruschetta G, Jin S, Liu ZW, Kim JD, Diano S. MC4R Signaling in dorsal raphe nucleus controls feeding, anxiety, and depression. Cell Rep 2020;33(2):108267.
[48] Sternson SM, Shepherd GM, Friedman JM. Topographic mapping of VMH → arcuate nucleus microcircuits and their reorganization by fasting. Nat Neurosci 2005;8(10):1356–63.
[49] Li L, Wyler SC, Leon-Mercado LA, Xu B, Oh Y, Swati, et al. Delineating a serotonin 1B receptor circuit for appetite suppression in mice. J Exp Med 2022;219(8).
[50] Atasoy D, Betley JN, Su HH, Sternson SM. Deconstruction of a neural circuit for hunger. Nature 2012;488(7410):172–7.

